Journal of Power Sources 183 (2008) 69–75

Contents lists available at ScienceDirect

Journal of Power Sources

journal homepage: www.elsevier.com/locate/jpowsour

A high conductivity $Cs_{2.5}H_{0.5}PMo_{12}O_{40}$/polybenzimidazole (PBI)/H_3PO_4 composite membrane for proton-exchange membrane fuel cells operating at high temperature

Ming-Qiang Li [a,*], Zhi-Gang Shao [b], Keith Scott [a]

[a] School of Chemical Engineering & Advanced Materials, Newcastle University, Newcastle NE1 7RU, United Kingdom
[b] Fuel Cell R&D Center, Dalian Institute of Chemical Physics, Chinese Academy of Sciences, Dalian 116023, China

ARTICLE INFO

Article history:
Received 5 February 2008
Received in revised form 21 April 2008
Accepted 27 April 2008
Available online 15 May 2008

Keywords:
Polyoxometalate
Proton-exchange membrane
PEM
High-temperature
Fuel cell
PBI

ABSTRACT

A high conductivity composite proton-exchange membrane $Cs_{2.5}H_{0.5}PMo_{12}O_{40}$ (CsPOM)/polybenzimidazole (PBI) for use in hydrogen proton-exchange fuel cells has been prepared. The CsPOM composite membrane is insoluble in water. The composite membrane doped with H_3PO_4 showed high-proton conductivity (>0.15 S cm^{-1}) and good thermal stability. ^{31}P NMR analysis has suggested the formation of a chemical bond between the CsPOM and PBI in the composite membrane. The performance of the membrane in a high-temperature proton-exchange membrane fuel cell (PEMFC) fueled with hydrogen was better than that with a phosphoric acid-doped PBI membrane under the same conditions and at temperatures greater than 150 °C. The CsPOM/PBI composite would appear to be a promising material for high-temperature PEMFC applications.

1. Introduction

The operation of proton-exchange membrane fuel cells (PEMFCs) at high-temperature and low-relative humidity provides several advantages over traditional lower temperature cells:

(i) Minimising anode catalyst poisoning caused by CO.
(ii) Fuel cell flooding is almost avoided.
(iii) The efficiency of fuel cell can be significantly improved due to the usable thermal energy generated.
(iv) The amount of noble metal catalyst can potentially be reduced due to fast reaction kinetics at high-temperature.
(v) Reactant gas humidification is not necessary.

Therefore, the development of a PEM, which has satisfactory proton conductivity at higher temperatures and low relative humidity, is of great importance in high-temperature PEMFC research and development [1–4].

Polybenzimidazole (PBI) has quite recently been used as a basis of intermediate temperature PEMFCs. Doping the PBI with phosphoric acid has lead to reasonably successful membranes with excellent thermo-chemical stability and good proton conductivity [5]. Poly(2,2-*m*-(phenylene)-5,5-bibenzimidazole), a commercial product, has a glass transition temperature of 425–435 °C and thus has good thermal stability for use in high-temperature PEMFCs. Another structure of PBI, named as AB-PBI, poly(2,5-benzimidazole), has provided good performance in PEMFCs [6].

Polyoxometalates, a class of molecularly defined inorganic metal oxide clusters, possess intriguing structures and diverse properties and are attracting attention as building blocks for functional composite materials; because of their nano-size characteristsics. The combination of inorganic building blocks with appropriate organic molecules has been used to develop a variety of polyoxometalates-based composite materials [7–11].

In this work we have blended PBI with a solid acid, $Cs_{2.5}H_{0.5}PMo_{12}O_{40}$ (CsPOM), which was insoluble in water, to form a composite membrane. The blend resulted in the formation of a chemical bond between PBI and CsPOM, which was indicated by ^{31}P NMR. The proton conductivity of CsPOM/PBI composite membrane was measured, and the physical–chemical characterizations of CsPOM/PBI/H_3PO_4 membrane evaluated. The test showed that the CsPOM/PBI composite membrane had a better performance than a PBI membrane in a high-temperature PEMFC.

* Corresponding author. Tel.: +44 191 2225747; fax: +44 191 2225747.
E-mail addresses: M.Q.Li@ncl.ac.uk, limingqiang918@sohu.com (M.-Q. Li).

0378-7753/$ – see front matter.
doi:10.1016/j.jpowsour.2008.04.093

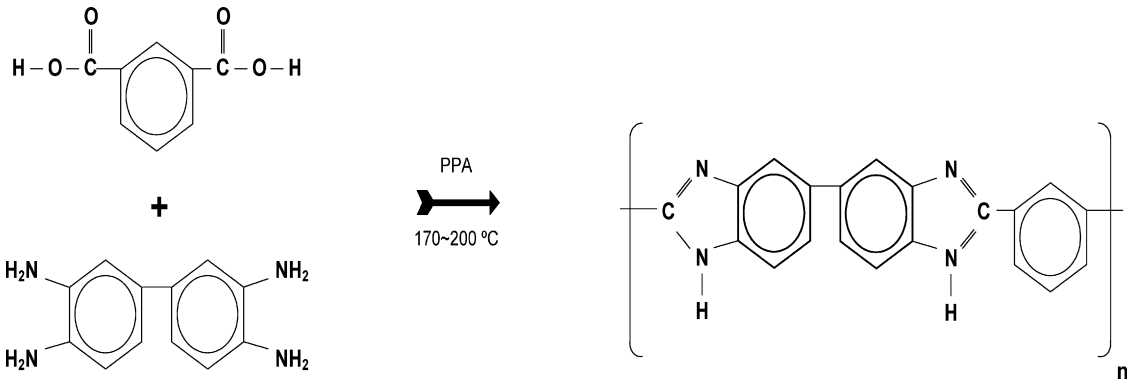

Scheme 1. Preparation of the PBI resin.

2. Experimental

2.1. Composite membrane preparation

PBI (poly[2,2′-*m*-(phenylene)-5,5′-bibenzimidazole was prepared from 3-3′-diaminobenzidine and isophtalic acid in polyphosphoric acid (PPA) by solution poly-condensation at temperatures between 170 and 200 °C, according to the reaction as shown in Scheme 1.

The PBI obtained had an inherent viscosity (IV) of 0.6–0.8 dl g^{-1} when measured in a concentration of 0.4 g of PBI in 100 ml of 97% sulphuric acid at 25 °C.

$Cs_{2.5}H_{0.5}PMo_{12}O_{40}$ was prepared from $H_3PMo_{12}O_{40}$ (Aldrich) and Cs_2CO_3 (Aldrich) according to published procedures [12–14]. In this procedure a solution of 0.815 g Cs_2CO_3 dissolved in 10 cm^3 water was added drop-wise to a solution of 3.65 g $H_3PMo_{12}O_{40}$ dissolved in 15 cm^3 water, to a final ratio of 1.25 (mol:mol). The resulting precipitate was recovered from the solution by evaporation at 55 °C and purified, by washing with de-ionised water and filtering, three times.

The composite membrane was prepared according to the following method. Firstly, the CsPOM inorganic powder was dispersed in a PBI-1-methyl-2-pyrrolidinone (NMP) solution with a mass ratio of PBI:CsPOM = 2:1 or 3:1. Secondly, the CsPOM/PBI composite membrane was synthesized by evaporating the NMP solvent at 120 °C for 2 h. Finally, the composite membrane was immersed in a H_3PO_4 aqueous solution (85 wt%) for 10 h at 25 °C for acid doping. In the acid doping step, 1.0 g of CsPOM/PBI composite membrane could absorb 2.0 g H_3PO_4. Before using the membrane, any residual H_3PO_4 on its surface was removed. Using the procedure described above, CsPOM/PBI composite membranes, doped with H_3PO_4, were prepared.

2.2. PBI membrane preparation

PBI powder (IV = 0.7 dl g^{-1}) was dissolved in *N*,*N*′-dimethylacetamide (DMAc) at a temperature of 250 °C (80 °C above the boiling point of DMAc) in an autoclave. In this procedure the autoclave was purged with nitrogen and heated gradually to 250 °C, whilst the pressure was increased to 6 bar. The temperature was then held at 250 °C for 5 h and the solution stirred to allow the majority of the polymer to dissolve. The solution was then poured onto an optical glass and kept in an oven at a temperature of 90–110 °C for 12 h to evaporate the solvent and form the membrane.

2.3. Membrane characterisation

The thermal stability of the composite membrane was determined using a high-resolution Pyris Diamond TGA, Thermo-

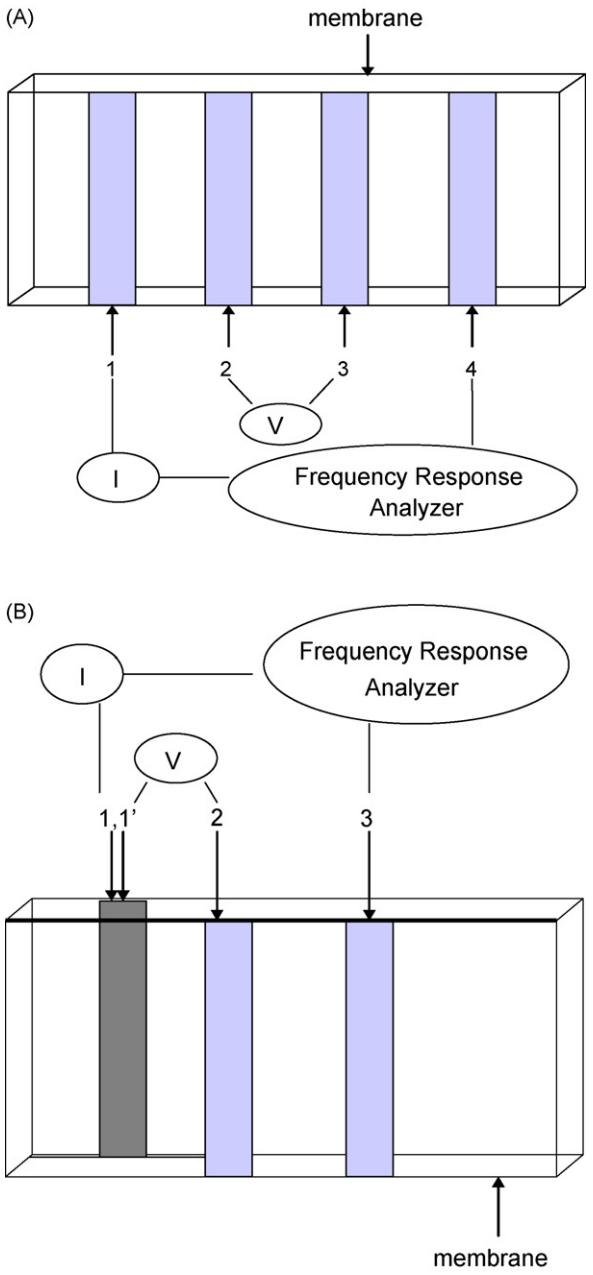

Fig. 1. Four point probe method to measure the surface conductivity and cross-section conductivity of membrane. (A) Four-point method for surface conductivity and B) four-point method for cross-section conductivity.

gravimetric Analyzer, made by PerkinElmer Instruments. The samples were heated, at a rate of 10 °C min^{-1}, from 30 to 800 °C, in a N_2 atmosphere.

The surface and cross-section conductivity of membrane were measured using a four-point probe and Frequency Response Analyzer (Voltech TF2000, UK) as shown in Fig. 1. The four-point method was used as it is superior to the two-point method, as it eliminates the probe resistance and resistance between the probe and the membrane surface. The technique involves four equally spaced probes in contact with the measured material; two of the probes are used to source current whilst the other two are used to measure the voltage drop. The membranes were cut into 1 cm × 5 cm strips and placed across four platinum foils with equal spacing of 0.5 cm. AC impedance measurements were carried out between frequencies of 1 and 20 kHz. The polymer membranes were held at the desired conditions of temperature and humidity for 3 h, to ensure steady state was achieved, and measurements were taken at 30 min intervals.

The ^{31}P NMR experiments were carried out on a Bruker AMX-300 spectrometer using a 10-mm static probe (Morris Instrument Inc.).

The surface and cross-section morphology of the composite membrane was measured by a JSM-6360LV (Japan) Scanning Electron Microscope.

2.4. Membrane electrode assemblies (MEA)

MEA were prepared as follows. Firstly, catalyst inks were prepared by blending carbon-supported catalysts (60% Pt on Vulcan XC-72, Etek Inc.) and the solution of PBI in DMAc (5%, w/w) and 1% (w/w) PVDF solution in DMAC for 12 h. The inks were cast onto a carbon-supporting layer covered with a gas diffusion layer (Etek Inc.). After 10 h at room temperature, the electrodes were heated at 150 °C for 1 h. Membrane electrode assemblies were made by hot pressing the anode and cathode onto the acid doped membranes at 150 °C and 0.1 ton cm^{-2} pressure for 10 min.

2.5. Fuel cell tests

To perform cell tests the MEA was in contact with high-density graphite blocks, impregnated with phenolic resin, into which were machined parallel gas flow channels. The active cross-section area of the membrane was 1.0 cm^2. The ridges between the channels provided electrical contact to the carbon electrodes and the total machined cross-sectional area, was taken as the active cell area. Electric cartridge heaters were mounted at the rear of the graphite blocks to maintain the desired cell temperature, which was monitored by thermocouples imbedded in the graphite blocks and controlled with a temperature controller. Gold-plated steel bolts were screwed into the blocks to allow electrical contact. Hydrogen and air were fed to the cell, at flow rates of 0.2 and 0.45 dm^3 min^{-1}, respectively. These flow rates were some 40 times excess of stoichiometric requirements at the maximum current obtained from the cell tests.

3. Results and discussion

Fig. 2 shows SEMs of the cross-section of the CsPOM/PBI composite membrane (a) and the PBI membrane (b). The net texture, shown in the image of the CsPOM/PBI composite membrane, is not found in that of the PBI membrane. This suggests that the CsPOM grains were inter-connected in the composite membrane. Therefore, proton conduction paths were established via the PBI polymer over the whole membrane and these proton conduction paths provide a possible interpretation for the high-proton conductivity of

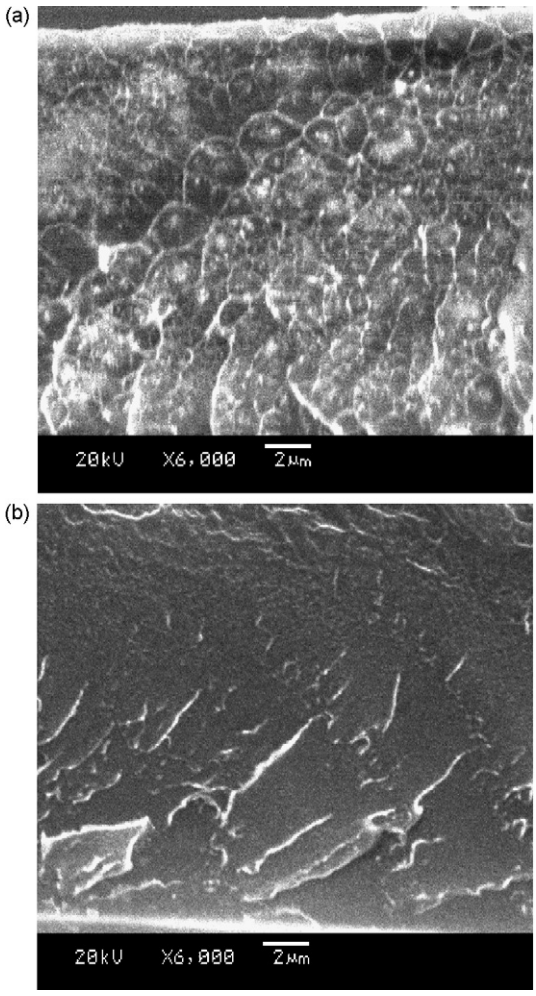

Fig. 2. SEM image of PBI/CsPOM composite membrane cross-section (a) and PBI membrane cross-section (b).

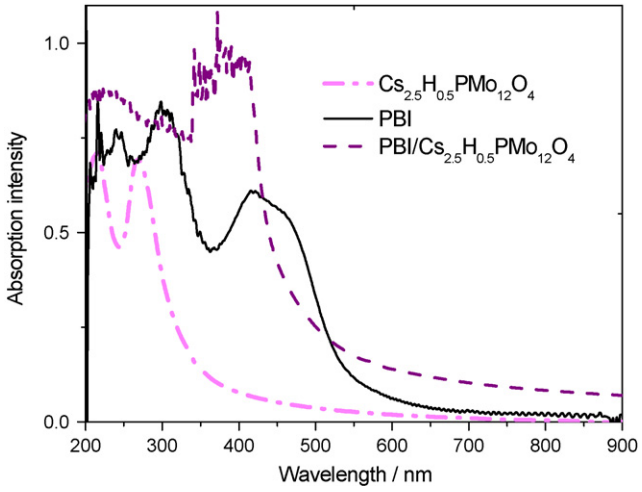

Fig. 3. UV–vis spectra of CsPOM, PBI and CsPOM/PBI composite membranes.

the composite membrane. A similar structure was observed in SEMs of zirconium phosphate (ZrP)/PBI membranes in which inorganic particles were encircled by polymer lines [15].

Fig. 3 shows the UV–vis spectra of the composite membrane, PBI and CsPOM. There was a wide absorption band near 350–450 nm,

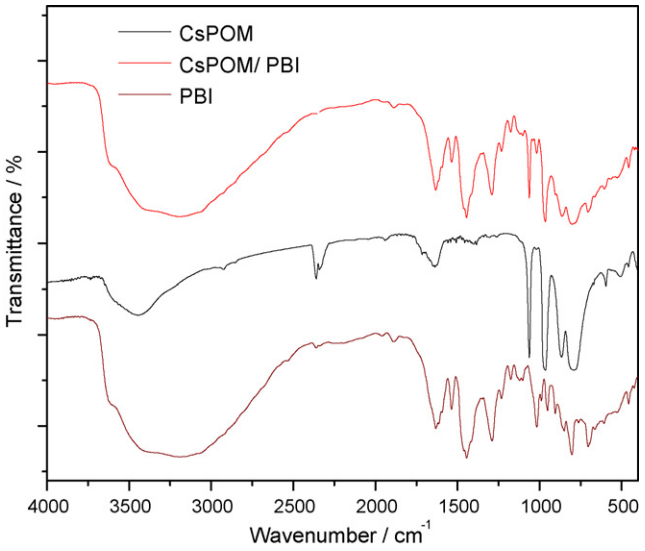

Fig. 4. Infrared spectra of composite membranes, PBI and CsPOM.

in the UV–vis spectra of the composite membrane. This was associated with the transfer absorption band of n–π in PBI, which shifted and increased due to the interaction between PBI and CsPOM. The infrared spectra of CsPOM (Fig. 4) shows the characteristic vibration bands of P=O (1063 cm^{-1}), Mo=O (938 cm^{-1}), Mo–O_b–Mo (889 cm^{-1}) and Mo–O_c–Mo (812 cm^{-1}). These characteristic vibration bands were also shown in the infrared spectra of CsPOM/PBI. The 3000–3700 cm^{-1} region of the spectrum of the CsPOM/PBI indicated the N—H stretch near 3400 cm^{-1} and the hydrogen-bonded N—H stretch at 3145 cm^{-1}. This was also seen in the spectrum of PBI.

Because ^{31}P NMR has good sensitivity and a wide chemical shift range, it is very sensitive to the valence of the P atom and the change of type, quantity and structure of atoms or groups associated directly with the P atom [16]. The ^{31}P NMR spectra of the CsPOM/PBI membrane, shown in Fig. 5, were thus used to study its structure. The peak, with a chemical shift of 7.6 ppm, may be attributed to the CsPOM. Another peak, with a chemical shift of 0.06 ppm, may be attributed to the CsPOM/PBI. The change of the chemical shift was associated with PBI which increased the electron density surrounding the phosphorus atom. The data suggest that a chemical bond may have been formed between CsPOM and PBI. Moreover, there was also some CsPOM independently trapped in the membrane.

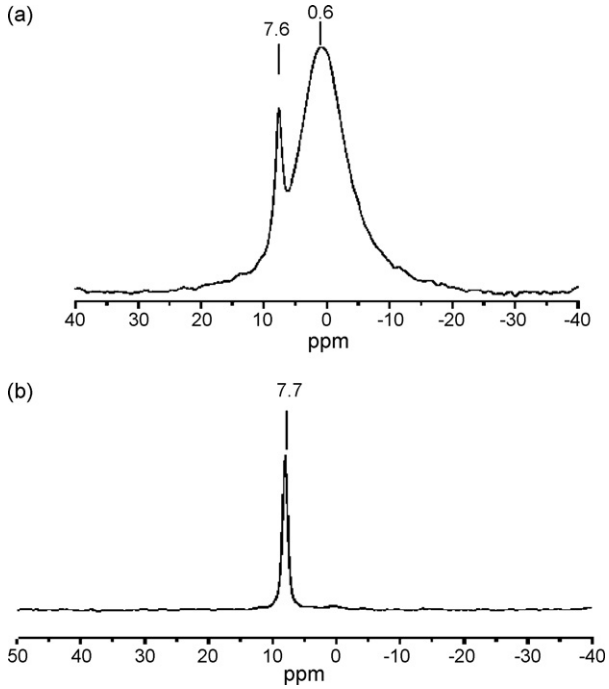

Fig. 5. ^{31}P NMR of CsPOM/PBI membrane (a) and CsPOM (b).

In addition, we tested the solubility of the membrane to further indicate bond formation. Pure PBI was soluble in DMAC whilst the PBI–CsPOM was insoluble in DMAC. This indicated the formation of a bond rather than just a blend of PBI with CsPOM.

Thermo-gravimetric analysis data of PBI, CsPOM, PBI doped with H_3PO_4 and CsPOM/PBI composite membranes doped with H_3PO_4 are shown in Fig. 6. Below temperatures of 100 °C, a rapid weight loss occurred with the PBI membrane due to water evaporation, whilst for PBI/H_3PO_4 and CsPOM/PBI/H_3PO_4 membrane, no obvious weight loss occurred, because of hygroscopic nature of H_3PO_4 and CsPOM. From 150 to 200 °C, PBI/H_3PO_4 and CsPOM/PBI/H_3PO_4 membranes experienced rapid weight loss, due to the evaporation of water in H_3PO_4. In the range of 230–340 °C, the decomposition of CH_2 organic components was responsible for the weight loss. At approximately 550 °C, the main chain of PBI started to decompose [17]. For CsPOM, evaporation of intra-molecular and inter-molecular water caused a rapid weight loss below 200 °C. The TGA data showed that the CsPOM/PBI composite membrane, doped with H_3PO_4 was stable below 230 °C, and thus its thermal stability meets with the requirements of high-temperature PEMFCs.

Fig. 7 shows the conductivity data of the PBI/H_3PO_4 membrane and the CsPOM/PBI/H_3PO_4 membrane, doped in phosphoric acid (H_3PO_4, 85%). From both the surface conductivity and cross-section conductivity, it is clear that the CsPOM/PBI/H_3PO_4 membrane had a higher conductivity than that of the PBI/H_3PO_4 membrane. This behavior can be attributed to a combination of the conductivities of CsPOM and phosphoric acid, and also to the increased phosphoric acid uptake caused by the CsPOM solid acid. We also compared the surface conductivity with cross-section conductivity for same membrane. Both the composite membrane and the PBI membrane had greater surface conductivities than cross-sectional conductivities; as a result of the membrane surface having more H_3PO_4 than the cross-section. The relatively high-proton conductivity of CsPOM/PBI/H_3PO_4 composite membrane indicates that it is a promising material for high-temperature PEMFC applications.

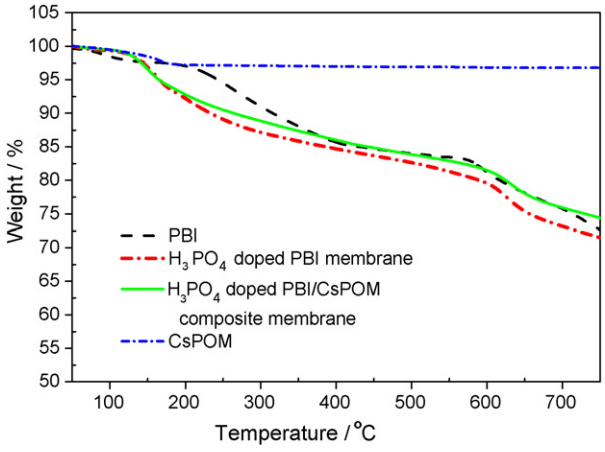

Fig. 6. TGA data of PBI, CsPOM, PBI/H_3PO_4 and CsPOM/PBI/H_3PO_4 composite membranes.

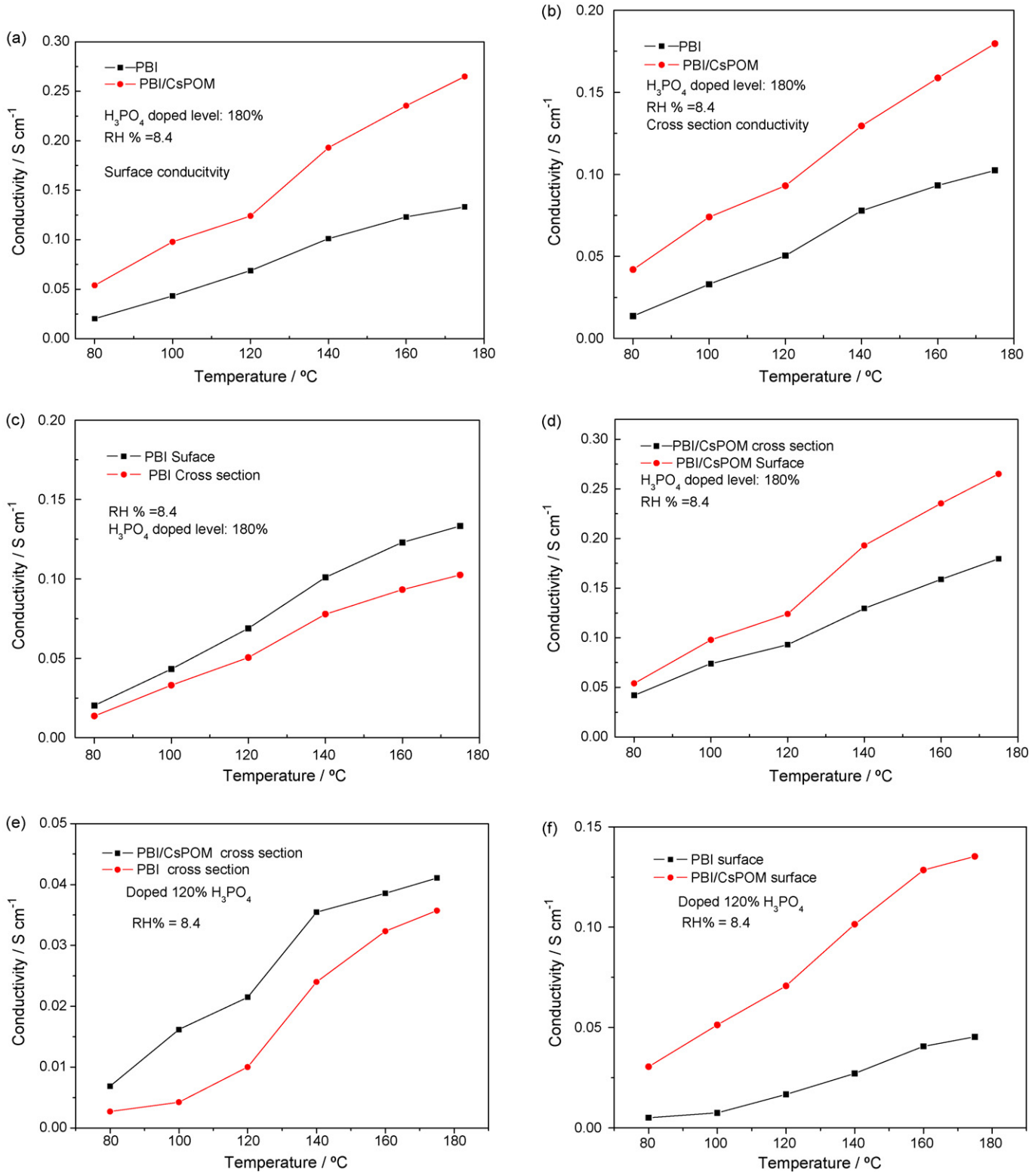

Fig. 7. Proton conductivity of CsPOM/PBI/H_3PO_4 composite membrane, PBI/H_3PO_4 membrane under a dry environment. Membrane thickness was identical for both materials. (a) Surface conductivity of CsPOM/PBI/H_3PO_4 and PBI/H_3PO_4 in 180% H_3PO_4 doping; (b) cross-section conductivity of CsPOM/PBI/H_3PO_4 and PBI/H_3PO_4 in 180% H_3PO_4 doping; (c) surface conductivity and cross-section conductivity of PBI/H_3PO_4; (d) surface conductivity and cross-section conductivity of CsPOM/PBI/H_3PO_4; (e) cross-section conductivity of CsPOM/PBI/H_3PO_4 and PBI/H_3PO_4 in 120% H_3PO_4 doping; and (f) surface conductivity of CsPOM/PBI/H_3PO_4 and PBI/H_3PO_4 in 120% H_3PO_4 doping.

Moreover, we also tested the conductivity of the CsPOM/PBI membrane without phosphoric acid. The conductivity of CsPOM/PBI membrane was 0.00004 S cm^{-1} at 150 °C and a relative humidity of zero. The low conductivity clearly shows that without doping it is not suitable for a high-temperature PEMFC.

Fig. 8 shows the typical performance of a H_2/O_2 fuel cell with the CsPOM/PBI membrane operated at 150 °C. With oxygen, cell

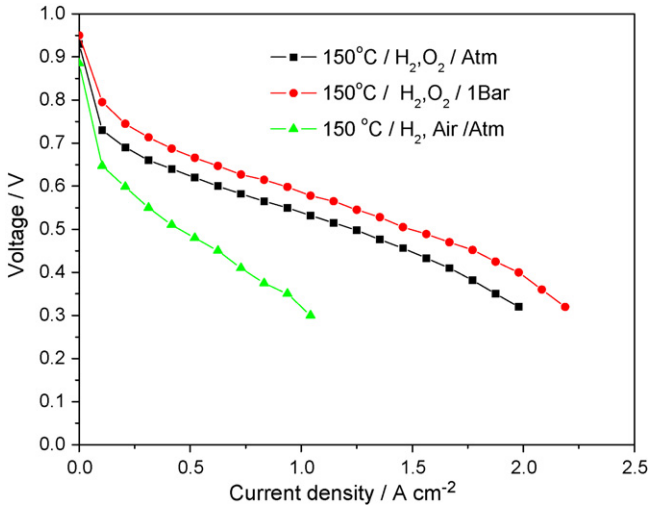

Fig. 8. Polarization and power density curves of a PEMFC with CsPOM/PBI/H_3PO_4 composite membranes at 150 °C with air and oxygen. PBI:CsPOM = 3:1, thickness: 30 μm Pt loading: cathode 0.81 mg cm^{-2}; anode 0.81 mg cm^{-2}; RH% = 0, H_3PO_4 doping level: 184%. Pt/C (60%):PVDF:PBI = 230:7:15.

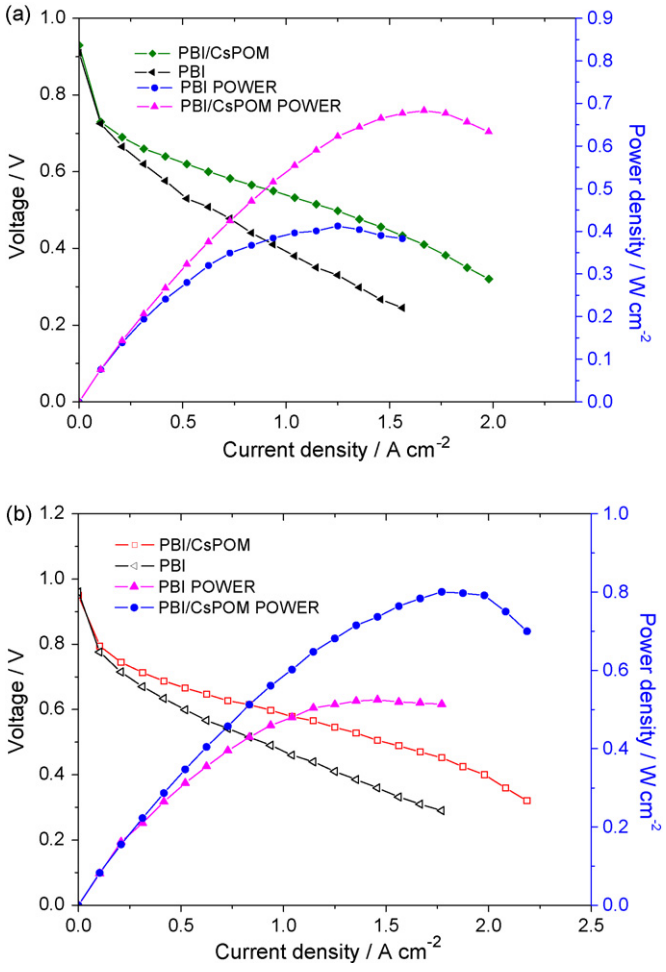

Fig. 9. The comparisons of CsPOM/PBI/H_3PO_4 composite membranes and PBI/H_3PO_4. PBI: CsPOM = 3:1, thickness: 30 μm; PBI thickness: 30 μm. Pt loading: cathode 0.81 mg cm^{-2}; anode 0.81 mg cm^{-2}; RH = 0%, H_3PO_4 doping level: 184%. Pt/C (60%):PVDF:PBI = 230:7:15; (a) polarization and power density curves of a PEMFC operated at 150 °C with. H_2/O_2 (150 °C, atmospheric pressure); (b) polarization and power density curves of a PEMFC operated at 150 °C with H_2/O_2 (150 °C, 1 bar).

Table 1
Cell voltage performance of fuel cells with CsPOM/PBI(1:3) with PBI membrane doped on 184% H_3PO_4 composite membrane (PBI:CsPOM = 3:1), thickness: 30 μm; PBI thickness: 30 μm; Pt loading: anode 0.81 mg cm^{-2}; cathode 0.81 mg cm^{-2}; catalyst layer: Pt/C (60 wt%):PVDF:PBI = 230:7:15

Current density (A cm^{-2})	0.75	0.85	1.0
Voltage of CsPOM/PBI/V	0.62	0.60	0.58
Voltage of PBI/V	0.53	0.51	0.48

Operation condition: 150 °C, H_2/O_2, 1 bar.

voltages of >0.6 V were achieved at a current density of 1.0 A cm^{-2}. With atmospheric air, the cell voltage was typically 0.5 V at 0.5 A cm^{-2} and a peak power density of some 330 mW cm^{-2} was achieved.

Fig. 9 and Table 1 compares the performance of fuel cells with the CsPOM/PBI composite and the PBI membranes. Open circuit potentials for the cells were around 0.95 V. Both cells exhibited significant activation polarization although the performance of the cell with the CsPOM/PBI composite membrane was significantly better than that with the PBI membrane at higher current densities, above 0.2 A cm^{-2}. This better performance was mainly attributed to the superior proton conductivity of the former and also the strong acid and water retention properties of the CsPOM. From the measured proton conductivities of the two materials, for a 30-μm thick membrane, at 1 A cm^{-2} there would be an approximate 0.15 V difference in voltage that corresponds with the observed cell polarization behavior. In addition, from the linear cell voltage vs. current density regions, assuming that these were only associated with the membrane resistance, gives values of cell conductivities of approximately 0.011 and 0.021 S cm^{-1} for the PBI and CsPOM/PBI cells which correspond approximately with the conductivity data.

Fig. 9b shows the typical influence of an increase in oxygen pressure on the fuel cell voltage and power density performance, at a temperature of 150 °C. The cell voltages produced with the composite membrane were much greater, by around 0.1 V, than those with the PBI membrane at high-current densities.

4. Conclusion

A composite proton-exchange membrane, made from CsPOM and PBI has been prepared. ^{31}P NMR analysis indicated the possible formation of a chemical bond between CsPOM and PBI in the composite membrane. The composite membrane, doped with H_3PO_4 had a high-proton conductivity; greater than that of a phosphoric acid doped PBI membrane and was thermally stabile above 200 °C. In fuel cell tests the CsPOM/PBI composite membrane, doped with H_3PO_4, gave superior performance to that of a phosphoric acid-doped PBI membrane and thus was suitable for high-temperature PEMFC applications.

Acknowledgement

The support of EPSRC is acknowledged through award no. EP/C002601; Supergen; fuel cell consortium.

References

[1] C. Yang, P. Costamagna, S. Srinivasan, J. Benziger, A.B. Bocarsly, J. Power Sources 103 (2001) 1–9.
[2] P. Costamagna, C. Yang, A.B. Bocarsly, S. Srinivasan, Electrochim. Acta 47 (2002) 1023–1033.
[3] Q. Li, R. He, J.O. Jensen, N.J. Bjerrum, Chem. Mater. 15 (2003) 4896–4915.
[4] D.A. Boysen, T. Uda, C.R.I. Chisholm, S.M. Haile, Science 303 (2004) 68–70.
[5] Q. Li, R. He, R.W. Berg, H.A. Hjuler, N.J. Bjerrum, Solid State Ionics 168 (2004) 177–185.
[6] J.A. Asensio, S.R. Borrós, P. Gómez-Romero, J. Membr. Sci. 241 (2004) 89–93.
[7] L. Xu, M.Q. Li, E.B. Wang, Mater. Lett. 54 (2002) 303–308.

[8] M.Q. Li, Z.G. Shao, H.M. Zhang, Y. Zhang, X. Zhu, B.L. Yi, Electrochem. Solid-State Lett. 9 (2006) 92–95.
[9] M.Q. Li, Z.G. Shao, H.M. Zhan, Electrochem. Solid-State Lett. 9 (2006) 60–63.
[10] P. Staiti, M. Minutoli, S. Hocevar, J. Power Sources 90 (2000) 231–235.
[11] J.A. Asensio, S. Borrós, P. Gómez-Romero, Electrochem. Commun. 5 (2003) 967–972.
[12] T. Nakato, M. Kimura, S. Nakata, T. Okuhara, Langmuir 14 (1998) 319–325.
[13] T. Okuhara, T. Nishimura, H. Watanabe, M. Misono, J. Mol. Catal. 74 (1992) 247–256.
[14] S. Tatematsu, T. Hibi, T. Okuhara, M. Misono, Chem. Lett. 6 (1984) 865–868.
[15] Y. Yamazaki, M.Y. Jang, T. Taniyama, Sci. Technol. Adv. Mater. 5 (2004) 455–459.
[16] M.Q. Li, X. Jian, Bull. Chem. Soc. Jpn. 78 (2005) 1575–1579.
[17] M. Kawahare, J. Morita, M. Rikukawa, K. Sanui, N. Ogata, Electrochim. Acta 45 (2000) 1395–1398.